

Kinetic Modelling of a Landfill Anaerobic Digestion Temperature in Relation to Multiphase Flow Across Unsaturated Porous Waste Media

 Aniekan Essienubong Ikpe*,  Victor Etok Udoh

Department of Mechanical Engineering, Akwa Ibom State Polytechnic, Ikot Osurua, PMB 1200 Nigeria

Received July 27, 2022; Accepted October 18, 2022

Abstract: Because an engineered landfill gas production unit is a closed system where organic waste is buried and compacted, there is need to understudy the kinetics under which gas evolves thereof. In this study, models were developed for multiphase flow across unsaturated porous waste media, semi-saturated and saturated media in a prototype landfill system. The anaerobic digestion temperature regime was kinetically Modelled for low, intermediate, and high landfill gas pressures as well as mass flow rates. The gas transport was modelled based on one dimensional transient basic differential equation while the biochemical kinetics was modelled based on Monod's Equation. The models which were developed for anaerobic digestion temperature at mesophilic range of 305, 309, 313, 317 and 321 K were narrowed down to multiphase flow across unsaturated porous organic waste media. The average maximum landfill gas pressures at low, intermediate, and high-pressure zones within the landfill confinements were recorded as 10.87, 13.31, 15.3, 17.8 and 20.4 KPa for the aforementioned mesophilic temperature along between flow distance of 0.0 and 0.045 m. Similarly, maximum mass flow rate of 1E-07, 1E-06, 1E-05, 1E-03 and 1E-01 kg/s were obtained for landfill gas at the same mesophilic temperature range. This indicated that landfill temperature is proportional to the average kinetic energy of the landfill gas densities and particles. Therefore, constant increase in the landfill temperature scaled up the heat rate per unit area of the landfill, which in turn served as a catalyst for microbial breakdown of organic waste for the generation and acceleration of gas flow within the landfill confinements.

Keywords: *Landfill, Leachate, Landfill gas, organic waste, porous media, Temperature.*

Introduction

Zhang *et al.* (2021) established a one-dimensional gas transport model for gas response in a landfill with layered new and old waste. The variation of gas permeability with depth, the anisotropy ratio of gas permeability, and settlement caused by waste biodegradation was considered in the model. Stratification of the unsaturated and saturated zones were also considered by distinguishing the difference in gas saturation. The maximum gas pressure occurred in the old waste layer near the boundary between new and old waste layers in the earlier period, but eventually moved to the bottom of landfill in the later period. The anisotropy ratio was observed as a more sensitive parameter influencing the distribution of landfill gas pressure. Ikpe *et al.* (2020a) investigated the biothermal variations in MSW landfill based on computational modelling. The results revealed that an increases in the landfill temperature stimulated gas particle movement, tending also to increase the pressure of the landfill gas, thereby, accelerating the rate of decomposition and adding more momentum to the gas particles to enable it spread more quickly within the confined system. Orhorhoro *et al.* (2018) investigated the effects of landfill gas flow trajectories at three distinct temperature phases (cryophilic temperature 50-150k, mesophilic temperature: 200-300k and thermophilic temperature 300-400k). Conservation mass equation was derived for solid, liquid, and gaseous phase of the landfilled waste matrix. The results reveal that the rate of landfill gas generation is dependent on the increase in temperature and pressure within the landfill system, usually causing subsurface pressures in the landfill to be higher than either the atmospheric pressure or indoor air pressure. This correlates with the findings of Ikpe *et al.* (2020b) from fuzzy modelling and optimization of anaerobic co-digestion process parameters for effective biogas yield from bio-wastes. Flow through waste solid matrix is usually considered as porous medium flow, generally simulated with Darcy's formulation (Bear, 1972), accounting also for capillary suction

*Corresponding: E-Mail: aniekan.ikpe@eng.uniben.edu;

and varying hydraulic conductivity as a function of liquid phase saturation. Measurements of solid waste porosity ranged from 28% to 33.5% (Beaven & Powrie, 1995) effective porosity and from 57.7% to 72.9% (Staub *et al.*, 2009) total porosity using laboratory scale tests). Once again, porosity of solid waste varies due to mechanical deformation and degradation. In the present study, however, a total porosity value of 50% was assumed to be constant in space and time. Kjeldsen and Fischer (1995) monitored the gas pressure in the old waste layer of Skellingsted landfill for 35 days, and results show that the variation of gas pressure in the landfill has a great influence on the composition of landfill gas. Gas pressure in Olinda and Louisiana landfills was measured for 3 and 5 days, and it was found that the measured pressure is influenced by fluctuations in atmospheric pressure (Spokas & Bogner, 1996; Bentley *et al.*, 2003). Gebert and Groengroft (2006) found that the amplitude of the gas pressure measured in two gas collection wells in an old German landfill exhibits a linear correlation with the amplitude of atmospheric pressure. Zhang *et al.* (2019) observed the gas pressure in the newly filled municipal solid waste (MSW) layer of the Wuxi landfill for more than 500 days, with results showing that the gas pressure varies with time, showing a single peak curve. The stratification of new and old waste layers is constantly occurring in operating landfills (Lefebvre *et al.*, 2000; Jang Kim, 2003). Gas breakthrough pressure and emission rate of unsaturated compacted clay were investigated by Chen *et al.* (2016), over a wide range of landfill gas pressures under various degrees of saturation, thicknesses, and degrees of compaction. Under a gas pressure of 10 kPa, a minimum of 0.4 m thick clay layer was able to prevent gas breakthrough at degree of saturation of about 60% or higher. Therefore, a thicker clay layer is required if clay degree of saturation is lower than 60%. For low degree of saturation (*i.e.*, 40%), degree of compaction had almost no influence on gas emission in the gas pressure range from 0 to 20 KPa. Therefore, gas breakthrough pressure of unsaturated compacted clay increased as the degree of saturation and thickness of clay increased. From the above report, several studies have been carried out on energy specific landfill system. However, this study is focused on the kinetic modelling of anaerobic digestion temperature regime in relation to multiphase flow across unsaturated porous waste media in a prototype landfill design framework.

Materials and Method

The 3D isometric landfill system was modelled using SOLIDWORKS 2018 software which is a solid modelling Computer Aided Design (CAD) as well as Computer Aided Engineering (CAE) tool that runs mainly on Microsoft Windows. The modelling steps started with 2D sketch, consisting of geometries such as arcs, points, conics, lines, splines and so on. Dimensions were added to the sketch to define the size and configuration of the geometry. Relations in the tool bar were used to define features such as parallelism, tangency, concentricity, perpendicularity among others. In the part assembly, sketches of individual parts were assembled together to form the intended solid model of the landfill system. The landfill data were obtained from a field prototype in the Faculty of Engineering, University of Benin, Nigeria. Materials used in the construction of the field prototype were used as a guide during selection of the landfill materials from SOLIDWORKS material library.

The landfill models as shown in Figure 1 and 2 incorporates all the functional materials needed for its operation. As shown in Figure 3, the gas extraction unit is modelled with four (4) cornered steel rods binned together with copper wire, and the annulus packed with granular materials (non-cancerous stone). Perforated gas extraction pipe is incorporated at the middle of the four (4) cornered steel rods to allow the flow and channelling of biogas generated from decomposing waste stream in the landfill to storage vessels. Borehole diameter for the gas extraction well is 0.20m while the gas extraction pipe diameter is 0.10m. Generally, landfill gas contains four major gases including CH₄, CO₂, N₂ and O₂ as well as moisture and other compounds in trace quantities, of which CH₄, (about 50-55%) and CO₂ (about 35-40%) accounts for the highest constituents. To obtain pure methane, which is the primary gas in a landfill gas, bio-filter is installed in the gas extraction pipe (see Figure 3) to purify and remove unwanted components from the raw landfill gas. The landfill model also incorporates perforated pipes buried horizontally (diameter of 0.10m and 0.40-0.50 m spacing) within the compacted waste layers and also within the granular layers (gravel layer) at the bottom of the landfill. The purpose is for transporting and channelling of leachate to a sizable trench (leachate collection sump) at a lower base of the landfill for extraction when necessary. The bottom and side walls of the system is modelled with bentonite clay (secondary liner) of low hydraulic conductivity (1×10^{-7} cm/s) to delay and control the rate of leachate percolation, while High Density Polyethylene (HDPE) liner (primary liner) is further modelled to align

properly with the surface of the bentonite clay liner to further prolong water retention in the landfill. The HDPE material specification was thickness of 2mm as presented by Ikpe et al. (2019). The model also incorporates polypropylene geotextile mat or geomembrane filter placed on the surface of the granular layer to separate solid particles from liquid content of the waste during decomposition.

Specifications of this material as presented by Ikpe *et al.* (2020c) are melting point temperature of 30°C, tensile strength between the range of 31.03-41.37MPa (ISO527), mass of 9613.75 g and thickness of 4.5mm. The waste permeability value was $3 \times 10^{-12} \text{m}^2$, porosity was 0.5, cover thickness was 0.3m, and the permeability of cover was $1 \times 10^{-13} \text{m}^2$. In evens of the primary and secondary liner failure, ground water monitoring probes is also incorporated in the model to detect the presence of leachate in ground water. The above descriptions of the landfill models are presented in Figure 1 and 2.

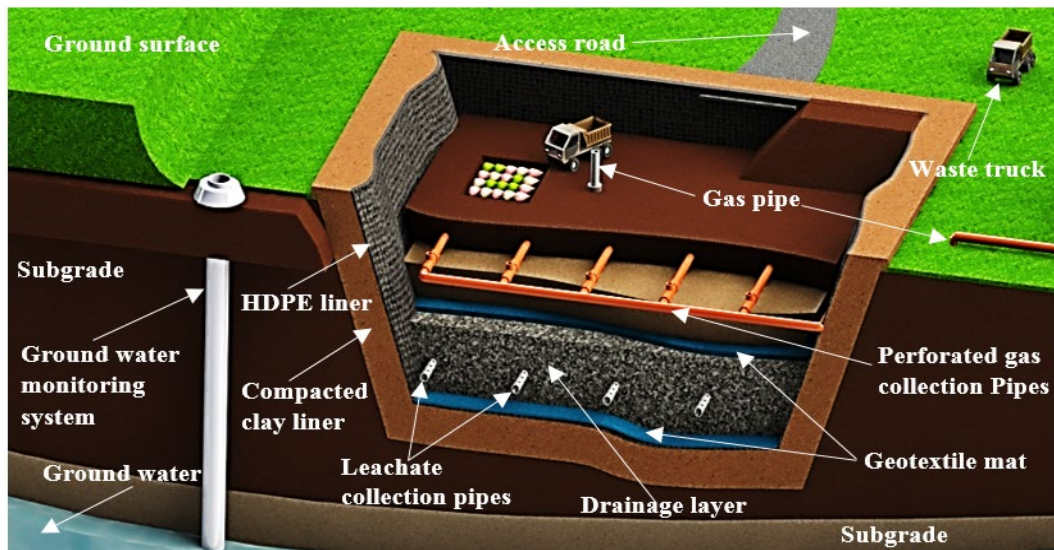


Figure 1. Cross sectional view of the landfill showing internal components

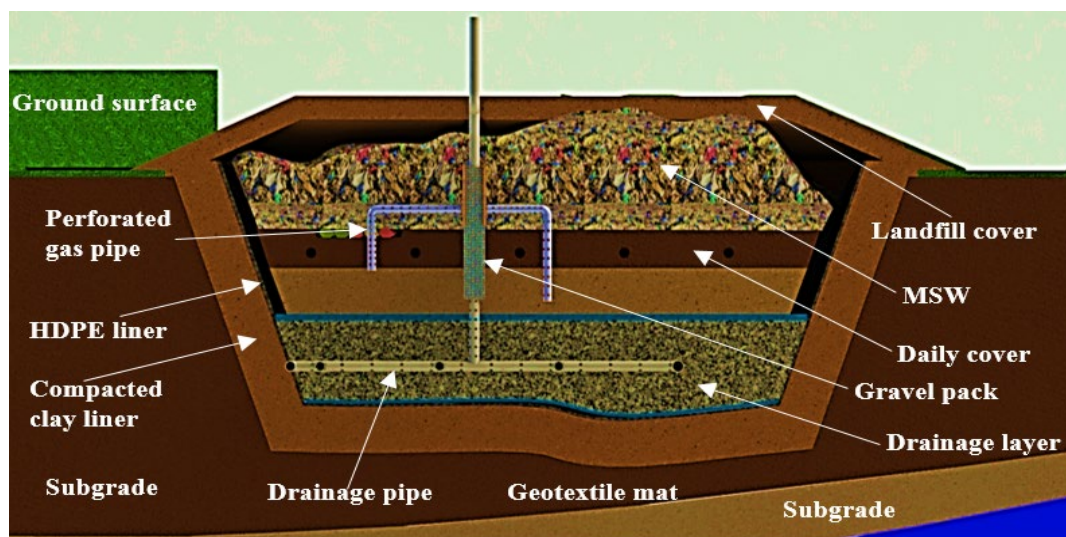


Figure 2. Cross sectional view of the landfill with MSW inside

The organic waste media was modelled for unsaturated, semi-saturated and saturated porous media using SOLIDWORKS 2018 software. The commercial CFD solver ANSYS Fluent 14.0 was used to simulate the complex anaerobic waste digestion-multiphase flow processes of the landfilled system at mesophilic temperature ranges of 305, 309, 313, 317 and 321 K. First-order spatial and temporal discretization was employed, while velocity-pressure coupling was achieved using “phase coupled SIMPLE” algorithm. The biochemical equations were computed implicitly while the flow model coupled with the biochemical process used the sink/source terms of the equations. Velocity magnitude

for flow regimes across porous media generally low, therefore, convergence properties for all partial differential equations were computerised low, in order to achieve convergence when all velocity components, mass and energy accuracy attain values of 10^{-12} . The following main assumptions were applied for model development:

- i. Gaseous phase flow in the landfilled solid waste matrix was described as unsaturated porous media multiphase flow.
- ii. Solid waste matrix was assumed to be rigid (non-deformable).
- iii. Flow was considered to be incompressible.
- iv. Thermal equilibrium was assumed between solid waste and surrounding or contained fluids.
- v. Biodegradable solid waste was assumed to be in fixed positions.
- vi. Biodegradation was assumed to occur in the liquid phase.
- vii. The pressure inlet boundary condition, which is mathematically described as a Dirichlet boundary condition for the relative pressure, was expressed as: $P_{inlet} = Pa$, where Pa is the relative pressure at the inlet. Similar boundary conditions were assumed for both the species mass transfer and temperature at inlet: $C_{inlet} = Ca$ and $T_{inlet} = Ta$, where Ca and Ta represent the values of species concentration and temperature at the inlet.
- viii. The pressure outlet boundary condition, which is a Dirichlet boundary condition for relative pressure, was assumed to be $P_{outlet} = Pb$, where Pb is the relative at the outlet. For the species mass transfer, zero flux boundary ($\frac{\partial C_{outlet}}{\partial n} = 0$) condition was assumed. For the temperature, Dirichlet boundary condition applied was: $T_{outlet} = Tb$, where Tb is the temperature value at outlet.
- ix. The impermeable rigid wall boundary condition, which is mathematically a Dirichlet boundary condition for the velocity assuming no-slip condition ($V_w = 0$ m/s). For the species mass transfer and temperature, zero flux boundary condition was applied: ($\frac{\partial C_w}{\partial n} = 0$ and $\frac{\partial h_w}{\partial n} = 0$).

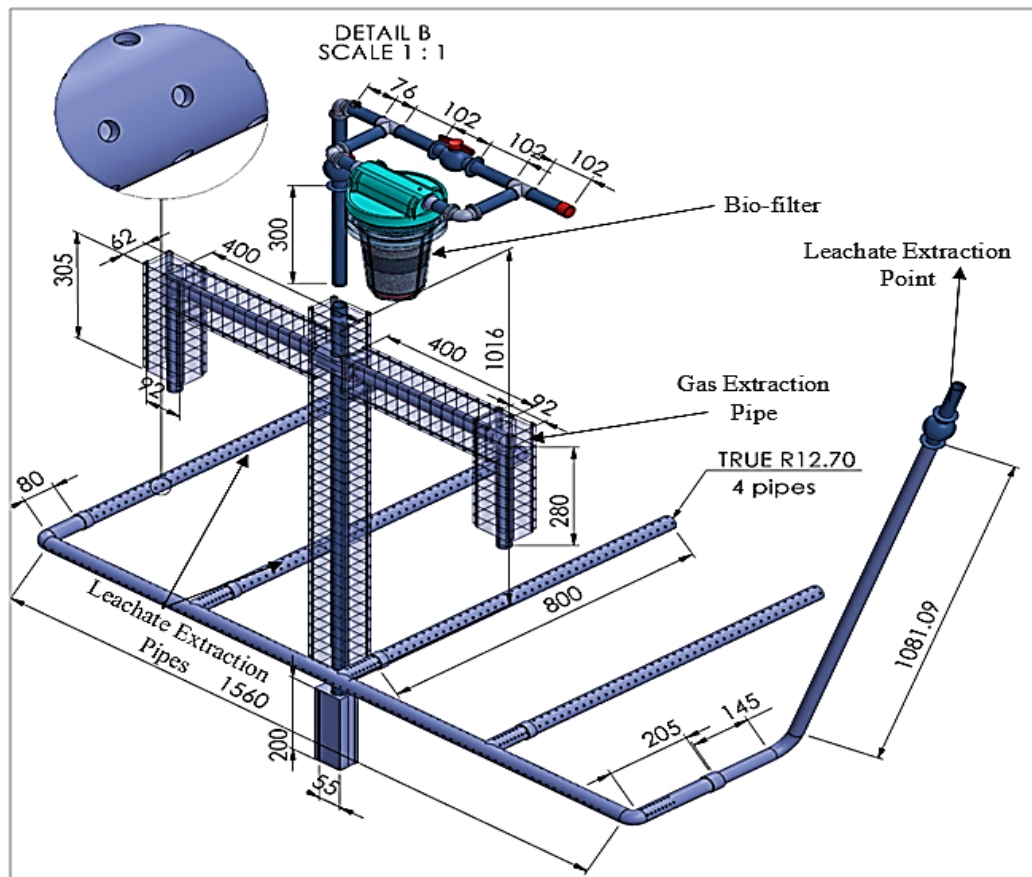


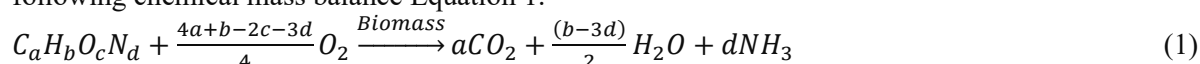
Figure 3. Layout of landfill leachate and gas extraction system

The kinetic modelling of anaerobic digestion temperature, mass flow rate and landfill gas pressure in relation to unsaturated porous media multiphase flow in a prototype landfill was achieved using the following properties in the gaseous, liquid and solid phases as well as the following flow parameters presented in Table 1.

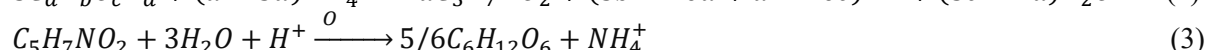
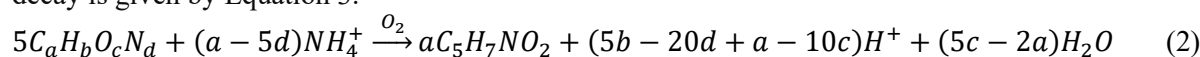
Table 1. Landfill properties in the gaseous, liquid and solid phases with flow parameters

Properties of the gas Phase	Minimum	Maximum
Thermal conductivity (W/mK)	0.015	0.038
Specific heat capacity (KJ/kgK)	600	2100
Density Fluid (Kg/m ³)	0.282	0.840
Velocity (m/s)	0	2198.108
Velocity (X) (m/s)	-195.020	195.130
Velocity (Y) (m/s)	-28.893	2197.940
Velocity (Z) (m/s)	-201.483	202.130
Temperature (K)	280.96	-
Mach Number	0	7.23
Vorticity (1/s)	22.226	71927.174
Molecular viscosity (Kg/m s)	1.7894 x10 ⁻⁵	1.7894 x10 ⁻⁵
Viscosity of gas mixture (Pa.s)	1.54x10 ⁻¹⁵	1.54x10 ⁻¹⁵
Relative Pressure (Pa)	-82543.53	-
Properties of Solid Phase (MSW)	Minimum	Maximum
Density (Kg/m ³)	140.2	220.8
Thermal conductivity (W/mK)	0.3	3.5
Specific heat capacity (KJ/kgK)	1000	2200
Residual saturation	0.03	0.03
Permeability of soil	1.0x10 ⁻¹⁵	1.0x10 ⁻¹⁵
Properties of liquid Phase	Minimum	Maximum
Liquid material (leachate)	-	-
Density (Kg/m ³)	3.2	5.1
Thermal conductivity (W/mK)	0.200	0.600
Specific heat capacity (KJ/kgK)	1000	3000
Dynamic viscosity (Kg/m s)	0.001003	0.001003
Temperature (Fluid) (K)	280.96	
Flow parameters		
Flow vectors direction	Normal to face	
Volume flow rate	0.1000 m ³ /s	
Viscous regime	Turbulent	
Turbulent intensity: 10%	10%	
Turbulent length scale	7% of the Hydraulic diameter	
Turbulent velocity scale	5% of the free steam velocity	

Tchobanoglous et al. (1993) described the kinetics of biodegradation in organic solid waste by the following chemical mass balance Equation 1.



Where the constants *a*, *b*, *c* and *d* are chemical compositions of the waste. The values for these constants have been estimated in numerous studies (Iannelli et al., 2005; Mavridis and Voudrias, 2021; and Komilis et al., 2012). The chemical formula for bacterial growth is given by Equation 2 (Stegenta-Dabrowska et al., 2022; Nayagum et al., 2009). The corresponding chemical equation for the biomass decay is given by Equation 3.



The kinetics of solid waste biodegradation and biomass production are connected with the relationship in Equation 4. Based on Monod's Equation, the biochemical kinetics in Equation 4 is expressed by the following relationship in Equations 5 and 6 (Qin et al., 2007; Lin et al., 2008; Higgins and Walker, 2001; Baptista et al., 2010).

$$S_s = \frac{dC_s}{dt} = \frac{S_B}{Y_s} = \frac{1}{Y_s} \frac{dC_B}{dt} \quad (4)$$

$$S_s = \frac{dC_s}{dt} = -k_m \frac{C_s}{K_s + C_s} C_B \quad (5)$$

$$S_s = \frac{dC_s}{dt} = -k' C_s \quad (6)$$

where S_s is the solid waste biodegradation rate, C_s is the concentration of biodegradable solid waste, t is the time, S_B is the biomass production rate, C_B is the biomass concentration in the waste stream, Y_s is the yield coefficient which connects kinetics of biodegradable solid waste and biomass, k_m is the maximum biodegradation rate in high biodegradable solids concentration and K_s is the half saturation constant for the solid waste. The factors that mostly influence the kinetics of biodegradation are temperature, moisture content in waste, particle size that prescribes the effective surface of solid matrix where biodegradation occurs, pH and so on (Baptista et al., 2010). Considering the aforementioned factors, Haug (1993) proposed the following equation:

$$S_s = \frac{dC_s}{dt} = -k' C_s = -k * k_{temp} * k_{mc} * k_{O_2} * k_{FAS} * k_{pH} * C_s \quad (7)$$

where k' is the effective/corrected biodegradation rate, k is the maximum biodegradation rate k_{temp} is the temperature correction function, k_{mc} is the moisture content correction function (dimensionless), k_{O_2} is the oxygen concentration correction function, k_{FAS} is the free air space correction function and k_{pH} is the pH correction function. Based on the cardinal temperatures T_{min} , T_{max} and T_{opt} , Rosso et al (1993) originally proposed the correction function expressed in Equation 8:

$$k_{temp} = \frac{(T - T_{max}) * (T - T_{min})^2}{(T_{opt} - T_{min}) * [(T_{opt} - T_{min}) * (T - T_{opt}) - (T_{opt} - T_{max}) * (T_{opt} + T_{min} - 2T)]} \quad (8)$$

where T_{min} is the minimum acceptable temperature, T_{max} is the maximum acceptable temperature, T_{opt} is the optimum temperature for the biodegradation of organic feedstock and T is the actual temperature. The expression in Equation 8 was employed by both Sole-Mauri et al. (2007) and Mason (2009), in studies conducted on biodegradable volatile solids degradation profiles in composting process.

According to the mass conservation law, the net mass of gas flowing into and out of the unit body plus the mass of gas production equal to the variation of gas mass in the unit body, which can be expressed in Equation 9 (Zhang et al., 2021). For unsaturated flow, Navier Stokes Brinkman equations for ‘Euler’ multiphase approach which is an extended Darcy’s model for simulation of momentum conservation in each control volume (Fytanidis and Voudrias, 2014) is given by Equation 10.

$$-\left(\frac{\partial \rho_g V_x}{\partial x} dx + \frac{\partial \rho_g V_y}{\partial y} dy + \frac{\partial \rho_g V_z}{\partial z} dz\right) dt + \rho_g Q G dx dy dz dt = \frac{\partial \rho_g \varepsilon S_g dx dy dz}{dt} dt \quad (9)$$

$$\frac{\partial \varepsilon a_q \rho_q \vec{V}_q}{\partial t} + \nabla \varepsilon a_q \rho_q \vec{V}_q \vec{V}_q = -\varepsilon a_q \nabla P + \nabla \varepsilon \bar{\tau} + \varepsilon a_q \rho_q \bar{g} - a_q^2 \frac{\mu_q}{k k_r} \vec{V}_q - \varepsilon a_q \nabla P_c \quad (10)$$

where ρ_g is the density of landfill gas, V_x , V_y and V_z are the volumes of landfill gas entering the unit body along directions O_x , O_y and O_z per unit time, ε is the total porosity of the medium, S_g is the gas saturation, a_q is the volume fraction of q phase, ρ_q is the density of q phase, \vec{V}_q is the Darcy velocity of q phase (air of water), P is the static pressure, $\bar{\tau}$ is the shear stress, g is the acceleration of gravity, μ_q is the dynamic viscosity of q phase, k is the intrinsic or saturated permeability of q phase, k_r is the formulation of relative permeability (dimensionless) derived by van Genuchten (1980). The capillary pressure term $\gamma a_q \nabla P_c$ is included only in the wetting phase (Mualem, 1976) where P_c is derived from van Genuchten (1980) formulation.

$$P_c = -\frac{\rho_w g}{\alpha} \left(\left(\frac{1}{S_e} \right)^{\frac{1}{\gamma} - 1} \right)^{1/\beta} \quad (11)$$

where ρ_w is the aqueous phase density, α and β are the van Genuchten constants ($\gamma = 1 - \frac{1}{\beta}$). Energy conservation equation for the kinetics of anaerobic digestion temperature regime is given by Equation (12).

$$\frac{\partial \varepsilon a_q \rho_q h_q}{\partial t} + \nabla \varepsilon a_q \rho_q h_q \vec{V}_q = \partial a_q \rho_q \frac{\partial P}{\partial t} + \varepsilon \bar{\tau}_q : \nabla \vec{V}_q - \nabla \varepsilon q_q + S_q \quad (12)$$

Where h_q is the specific enthalpy of q phase and S_p is the sink/source term of energy. The heat exchange between the different phases is derived from Equation 13.

$$Q_{pq} = h_{pq}(T_p - T_q) \quad (13)$$

where Q_{pq} is the heat transfer across the phases, T_p is the temperature of p phase, T_q is the temperature of q phase and h_{pq} is the volumetric heat transfer coefficient between the phases p and q derived as a function of Nusselt number (Ranz & Marshall, 1952). One dimensional transient basic difference equation of gas transport in MSW matrix is given by Equation 14. Equation 15 is the equation of one-dimensional transient difference scheme for gas transport in a landfill (Zhang et al., 2021).

$$\frac{K_{gz}}{u_g} \frac{\partial^2 P_g}{\partial z^2} + \frac{1}{u_g} \frac{\partial K_{gz}}{\partial z} \frac{\partial P_g}{\partial z} + \rho L_o \sum_{i=1}^3 w_i \frac{AG_i}{BG_i} (t + D_{Gi})^{-\frac{1+D_{Gi}}{BG_i}} -$$

$$nS_g \left\{ \begin{aligned} &1 + \frac{1}{e_0+1} \left[e_0 - C_c 1g \left(1 + \frac{t}{t_D} \right) + 1 \right] \frac{A_{Gi}t}{BG_i} e^{-\frac{t}{BG_i}} \\ &+ \frac{C_c}{(e_t+1)(t+t_D)1n 10} \left[1 - A_{Gi} * B_{Gi} \left(-\frac{t}{BG_i} e^{-\frac{t}{BG_i}} + 1 - e^{-\frac{t}{BG_i}} \right) \right] \end{aligned} \right\} = \frac{nS_g}{P_{atm}} \frac{\partial P_g}{\partial t} \quad (14)$$

$$f_{G1} \frac{P_{gk-1}^t - 2P_{gk}^t + P_{gk+1}^t}{h_z^2} + f_{G1} \frac{P_{gk+1}^t - P_{gk-1}^t}{2h_z} + f_{G3} \left(\rho L_o \sum_{i=1}^3 w_i \frac{AG_i}{BG_i} (t + D_{Gi})^{-\frac{1+D_{Gi}}{BG_i}} - \right) = f_{G4} \frac{P_{gk}^t - P_{gk}^{t-1}}{\tau} \quad (15)$$

where e_0 is the initial void ratio, e_t is the void ratio at time t , h_z is the step length in the vertical direction, τ is the step length of time, A_{Gi} is the parameter related to gas production rate, B_{Gi} is the time of peak gas production rate, D_{Gi} is the length of time that the waste has been degraded to produce gas. The liquid flow and landfill gas transportation in landfills are estimated according to the equations of mass conservation for leachate and landfill gas in Equations 16a and 16b.

$$\rho_w \frac{\partial}{\partial t} (nS) = \rho_w \nabla \cdot \left[\frac{k_{iw}k_{rw}}{\mu_w} \nabla \cdot (u_w + \rho_w g_z) \right] + f_w \quad (16a)$$

$$\frac{\partial}{\partial t} [\rho_g n(1 - S)] = \nabla \cdot \left[\frac{k_{ig}k_{rg}}{\mu_g} \nabla \cdot (\rho_g u_g + \rho_w g_z) \right] + f_g \quad (16b)$$

where: n is the porosity, S is the liquid saturation, r_w and r_g are the density of liquid and gas, r is the partial differential operator, k_{iw} and k_{ig} are the intrinsic permeability for liquid and gas, k_{rw} and k_{rg} are the relative permeability functions for liquid and gas phase which can be estimated via the van-Geunchten model (van Genuchten, 1980), μ_w and μ_g are the dynamic viscosities of liquid and gas, u_w is pore water pressure, u_g is pore gas pressure. The mass conservation equation for liquid phase (Equation 16a) and gas phase (Equation 16b) can be further expressed as shown in Equation 17 and 18. The governing equation of solute migration is expressed in Equation 19 (Liu et al., 2021).

$$-\rho_w n \frac{\partial s}{\partial s} \frac{\partial u_w}{\partial t} + \rho_w n \frac{\partial s}{\partial s} \frac{\partial u_g}{\partial t} + \rho_w S \frac{\partial n}{\partial t} = \rho_w \nabla \cdot \left[\frac{k_{iw}k_{rw}}{\mu_w} \nabla \cdot (u_w + \rho_w g_z) \right] + f_w \quad (17)$$

$$\rho_g n \frac{\partial s}{\partial s} \frac{\partial u_w}{\partial t} + \left[\frac{n(1 - S)M}{RT} - \rho_g n \frac{\partial S}{\partial s} \right] \frac{\partial u_g}{\partial t} + \rho_g (1 - S) \frac{\partial n}{\partial t} = \nabla \cdot \left[\frac{k_{ig}k_{rg}}{\mu_g} \nabla \cdot (\rho_g u_g) \right] + f_g \quad (18)$$

$$nS \frac{\partial c_i}{\partial t} - nc_i \frac{\partial s}{\partial s} \frac{\partial u_w}{\partial t} + nc_i \frac{\partial s}{\partial s} \frac{\partial u_g}{\partial t} + c_i S \frac{\partial n}{\partial t} = -\nabla \cdot (c_i v_w) + \nabla \cdot (D_i \nabla c_i) + f_c^i \quad (19)$$

where s is the suction, u is the vertical displacement of a landfill, M is the molecular weight of landfill gas, R and T are the ideal gas constant and temperature, v_w is the fluid velocity of liquid, D_i are diffusion coefficients of volatile fatty acids and methanogen. Viscosity of the gas mixture can be expressed as a function of the viscosities of individual gases (Poling *et al.*, 2001), given by Equation 20. Durmusoglu (2002) expressed the mass balance equation for the liquid and gas phase relation given by equation 21 and 22. The settlement of waste stream in the landfill can be estimated based on vertical volumetric strain of MSWs which is expressed in Equation 23.

$$\varphi_{ij} = \frac{\left[1 + \left(\frac{\mu_i}{\mu_j} \right)^{1/2} \left(\frac{M_j}{M_i} \right)^{1/4} \right]^2}{\sqrt{8} \left(1 + \frac{M_i}{M_j} \right)^{1/2}} \quad (20)$$

$$nS_l\rho_l\beta\frac{\partial P_l}{\partial t} + \rho_l n\frac{\partial S_l}{\partial t} + \rho_l S_l\frac{\partial V_s}{\partial z} + \rho_l S_l\frac{\alpha^* Y}{\rho_s} = \frac{\partial}{\partial z}\left[\frac{\rho_l k_l}{\mu_l}\left(\frac{\partial \rho_l}{\partial z} - \rho_l g\right)\right] \quad (21)$$

$$n(1-S_l)\frac{\bar{M}}{R\phi}\frac{\partial P_g}{\partial t} - \rho_g n\frac{\partial S_l}{\partial t} + \rho_g(1-S_l)\frac{\partial V_s}{\partial z} + \alpha^*\left(\frac{Y\rho_g(1-S_l)}{\rho_s} - 1\right) = \frac{\partial}{\partial z}\left[\frac{\rho_g k_g}{\mu_g}\left(\frac{\partial P_g}{\partial z} - \rho_g g\right)\right] \quad (22)$$

$$\varepsilon_z(\sigma', t) = C'_c \log \frac{\sigma'}{\sigma'_0} + \left[\varepsilon_{dc}(\sigma'_0) + (C'_\infty - C'_c) \log \frac{\sigma'}{\sigma'_0}\right] (1 - \exp(-C_s t)) \quad (23)$$

$$\sigma' = \sigma_T - [Su_w + (1-S)u_g] \quad (24)$$

where: $\varepsilon_z(\sigma', t)$ is the vertical volumetric strain of MSWs having a filled age of t under the effective stress σ' , C'_c and C'_∞ are the compression ratios for placed fresh MSW and fully decomposed MSW, σ_T is the total stress, σ'_0 is the pre-consolidation pressure, $\varepsilon_{dc}(\sigma'_0)$, is the sum of ultimate volumetric strains of decomposition compression and mechanical creep under pre-consolidation pressure and C_s is the secondary compression rate constant. Based on the finite-line source theory, Zeng *et al.* (2002) proposed the analytical equation for temperature response in the ground as:

$$\theta(r, z, t) - \theta_0 = \frac{q_l}{4\pi k} \int_0^H \frac{\operatorname{erfc}\left(\frac{\sqrt{r^2+(z-h)^2}}{2\sqrt{\alpha t}}\right)}{\sqrt{r^2+(z-h)^2}} - \frac{\operatorname{erfc}\left(\frac{\sqrt{r^2+(z+h)^2}}{2\sqrt{\alpha t}}\right)}{\sqrt{r^2+(z+h)^2}} dh \quad (25)$$

where H is the depth and erfc is complementary error function. Municipal solid waste is a porous medium with pore spaces between irregularly shaped solid grains. Analytical equations applicable to heat conduction in porous media is given by Equation 26 (Yang, 2016).

$$\begin{cases} (1-\phi)\rho_s c_s \frac{\partial \theta_s}{\partial t} = (1-\phi)\nabla \cdot (k_s \nabla \theta_s) \\ \quad + (1-\phi)Q_s + h(\theta_f - \theta_s) \\ \phi\rho_f c_f \frac{\partial \theta_f}{\partial t} + (\rho_f c_f)q_f \cdot \nabla \theta_f = \phi\nabla \cdot (k_f \nabla \theta_f) \\ \quad + (1-\phi)Q_f + h(\theta_s - \theta_f) \end{cases} \quad (26)$$

where θ_s and θ_f are the solid and fluid temperatures, ρ_s and ρ_f are the densities of solid and liquid phases c_s and c_f are specific heat capacities of solid and liquid phases, k_s and k_f are heat conductivities, Q_s and Q_f are sources for liquid phases, ϕ is the landfill waste porosity and h is the exchange heat transfer coefficient. However, the constitutive equations for heat transfer in porous media is given by Equation 27 (Nield and Bejan, 2006).

$$\begin{cases} (1-\phi)\rho_s c_s \frac{\partial \theta_s}{\partial t} = (1-\phi)k_s \nabla^2 \theta_s + h(\theta_f - \theta_s) + (1-\phi)Q_s \\ \phi\rho_f c_f \frac{\partial \theta_f}{\partial t} + \rho_f c_f q_f \cdot \nabla \theta_f = \phi k_f \nabla^2 \theta_f - h(\theta_f - \theta_s) + \phi Q_f \end{cases} \quad (27)$$

The time measured since the first layer of waste was deposited in the landfill is given by Equation 28.

$$T = T_0 + Y\frac{T_f}{D} + T_{g+}F_g \quad (28)$$

where D is the total landfill depth, T_0 is the time elapsed since the landfill was capped, T_f is the total time to fill the landfill, and T_s is the time for gas production to commence. The governing equation of landfill gas flow is given by Equation 29 while the landfill gas flow velocity (v_a) is given by Equation 30 (Feng *et al.*, 2009).

$$\frac{\partial(n\rho_a S_a)}{\partial t} + \nabla(\rho_a v_a) = F_g \quad (29)$$

$$v_a = -\frac{kk_{ra}}{\mu_a} (\nabla P_a + \rho_a g \eta) \quad (30)$$

where ρ_a is the gas density, S_a is the gas saturation, F_g is the source phase, k is the intrinsic permeability, k_{ra} is the gas relative permeability.

Results and Discussion

Effective resistance to gas flow in landfill systems is caused by permeability ratios between the various medium layers and spacing between perforated cross-sections. A no flux boundary condition is equivalent to an additional layer of zero permeability and thus infinite ratios for all other layers. Compacted waste layers with very low permeability will result in singularity with no flux conditions. The two reliable control measures are experimental determination of permeability ratios and aperture density. The thermodynamics and flow kinetics in a landfill gas involves no excessive pressure or temperature, and low Reynolds and Mach numbers (Nec and Huculak, 2010). Most landfills are

generally considered as landfills with a homogeneously unsaturated waste layer (Nastev et al., 2001; Lu et al., 2019) or a continuously placed waste layer (Li et al., 2012; Li et al., 2013). Since the voids in MSW landfills are not completely filled by the liquid phase, the presence of the gas phase reduces the volume of medium available for liquid flow in an unsaturated medium. When the gas and liquid phases flow together through a porous medium, saturations of the phases are less than unity ($S_l + S_g = 1$). The extent of waste compaction plays a vital role in the degree of saturation of waste in the landfill system. Hydraulic conductivities of the unsaturated, semi-saturated and saturated porous waste media were 1×10^{-7} m/s, 1×10^{-9} m/s and 1×10^{-12} m/s respectively as shown in Figures 4-6. The analysis mainly focused on multiphase flow across unsaturated porous waste media because, waste in landfill systems is rarely completely saturated since majority of the flow occur in the unsaturated phase above leachate table. Even in semi-saturated waste media, the formation of landfill gas creates bubbles of gas within the void space, indicating that the waste media is not fully saturated. However, in events where the organic waste media is completely saturated, gas becomes entrapped in the waste media, thereby, leading to clogging of internal gas extraction pipes and interruption in the gas flow rate.

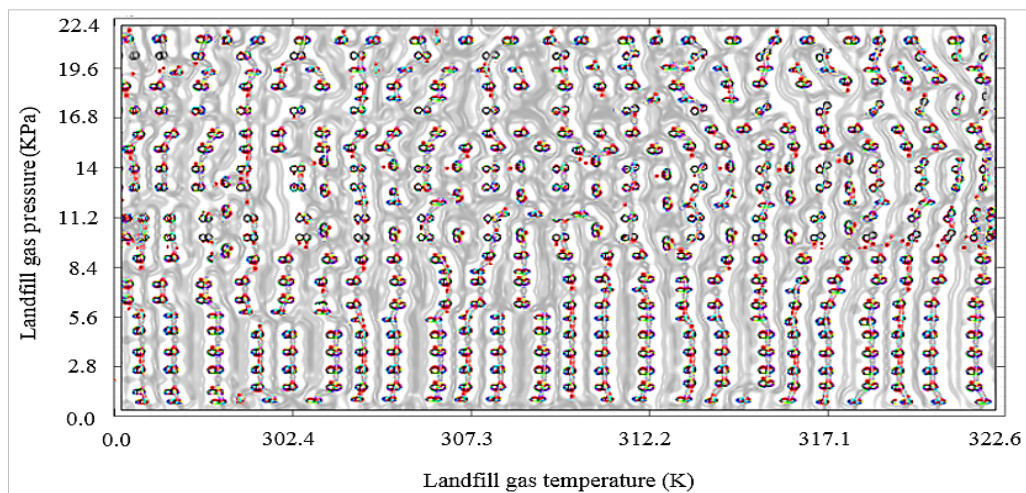


Figure 4. Unsaturated porous media with Hydraulic conductivity of 1×10^{-7} m/s

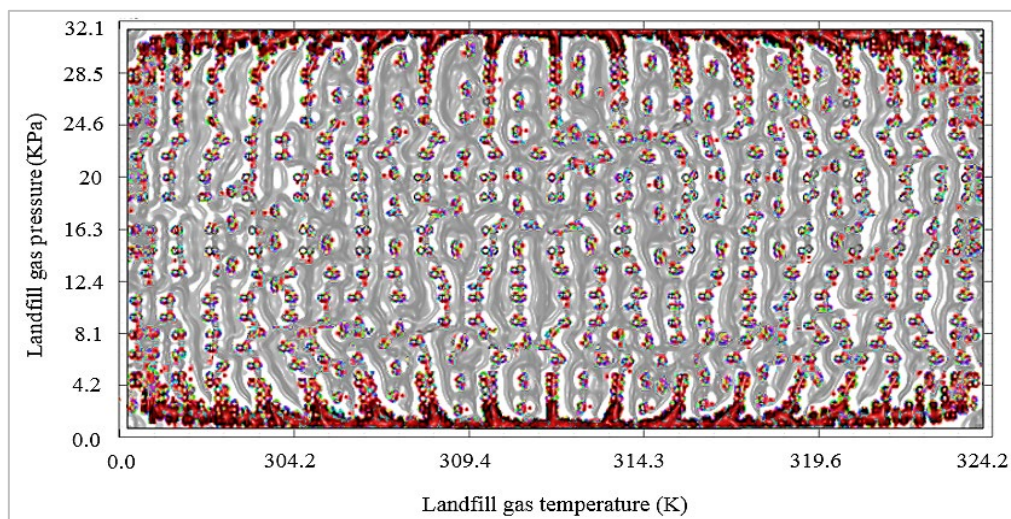


Figure 5. Semi-saturated porous media with hydraulic conductivity of 1×10^{-9} m/s

The white space indicated in Figure 4-6 signifies the pore spaces or drainage holes within the waste media. The said pore spaces are much in Figure 4, implying that the hydraulic conductivity (1×10^{-7} m/s) of the waste media is low, but enough for leachate and landfill gas can adequately flow through. Compared to Figure 4, the pore space (represented by white colour or colourless portion) between the compacted wastes media in Figure 5 is less, implying that the hydraulic conductivity (1×10^{-9} m/s) of the waste media is very low, but leachate and landfill gas can still manage to flow through but not

adequately. The pore space (represented by white colour or colourless portion) between the compacted waste media in Figure 6 is barely seen, as the hydraulic conductivity (1×10^{-12} m/s) of the waste media is extremely low, and leachate as well as landfill gas can hardly flow through. This indicates that the saturated porous media with hydraulic conductivity of 1×10^{-12} m/s looks non-porous, but not impervious, as such, the movement of leachate and landfill gas within the waste layers are almost but not completely restricted. Thus, a given landfill system operating under such condition is likely to fail in terms of not being able to give off gas as the other conditions in Figure 4 and 5 would. This can occur as a result of very low hydraulic conductivity within the waste media, hampering the pressure and mass flow rate of landfill gas and seeping tendency of the leachate into micro-pores and surrounding waste media within the system. This can also be due to clogging of the drainage systems or collapse of leachate transportation pipes as well gas channelling pipes, thereby, preventing the gas flow rate and leachate transport from functioning effectively. This may also take place due to the presence of excessive leachate in the system which can have a negative influence on microbial activities, thereby causing the organic substrate to soar or loose nutritional value for the microorganisms.

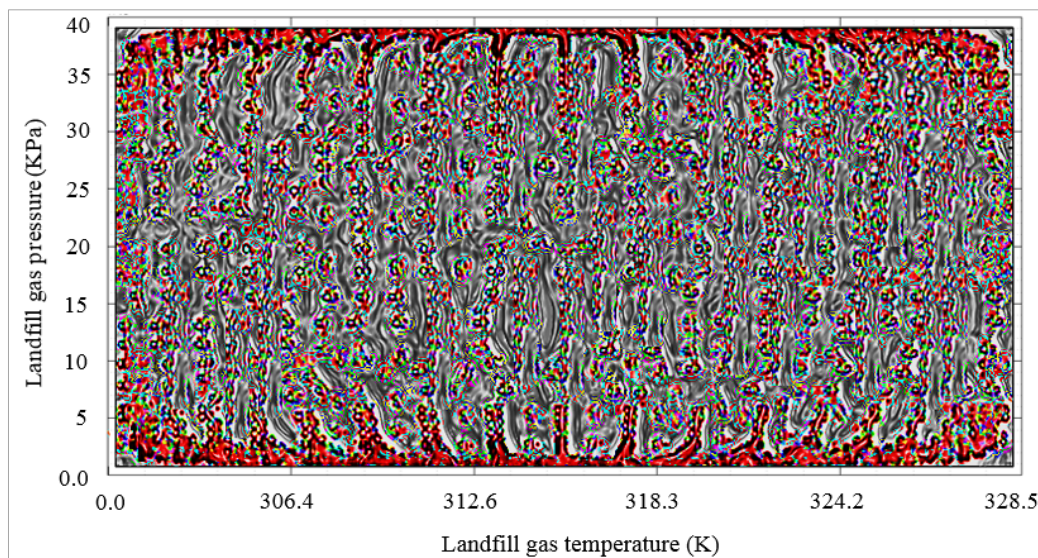


Figure 6. Saturated porous media with hydraulic conductivity of 1×10^{-12} m/s

Studies have also shown that high waste compaction may not be ideal for some landfills such as landfills with high moisture content or bioreactor landfill with leachate circulation, as it could be difficult for leachate to flow through the highly compacted waste layers that are more or less saturated and therefore causing pore pressure build-ups (Khalil *et al.*, 2014). However, Buivid *et al.* (1981) noted that higher compaction under well-mixed static landfill condition yielded higher methane gas volume. Hydraulic conductivity of a saturated waste is defined by Darcy's law and has the same unit as that of velocity. Hydraulic conductivities obtained from the field design in this study were in the range of 4.7×10^{-6} and 1×10^{-2} m/s. Hydraulic conductivity of MSW reported in literature vary approximately between 1.7×10^{-4} and 2.0×10^{-4} m/s (Beaven and Powrie, 1995), 4.7×10^{-7} and 9.6×10^{-4} m/s (Chen and Chynoweth, 1995), 3.9×10^{-7} and 6.7×10^{-5} m/s (Burrows *et al.*, 1997), 5.7×10^{-8} and 1.9×10^{-7} m/s (Jain *et al.*, 2006). However, effective porosities obtained from the field design in this study was used to determine the degree of saturation for MSW in prototype landfill presented in this study, which were in the range of 41.2-73.6%. Effective porosities of MSW reported in literature vary approximately between 1.5 and 14.4% and total porosity between 45.5 and 55.5 % (Hudson *et al.*, 2004), 47 and 57% (Zeiss, 1997), 48 and 51% (Olivier and Gourc, 2007), 45 and 62% (Stoltz & Gourc, 2007).

Figure 7 depicts the landfill models for gas pressure and mass flow rate at inactive state. Therefore, gas pressure and mass flow rate values for these models at inactive state are zero. The landfilled waste media is still undergoing hydrolysis, the conversion of polymetric organic matter (polysaccharides, lipids, proteins) to monomers (sugar, fatty acids, amino acids) by hydrolases secreted on the waste media by microorganisms. Heat and leachate are integral part of hydrolysis process even as decomposition, gas production as well as flow across the porous media (Sikora, 2017). At the end of hydrolysis, the next

process in the anaerobic digestion of landfill waste is known as acidogenesis. In this process, the products of hydrolysis are converted to non-gaseous short-chain fatty acids, alcohols, aldehydes and gases such as carbon dioxide and hydrogen. In the third stage known as acetogenesis, the non-gaseous products are further oxidized into hydrogen, carbon dioxide and acetate via syntrophic degradation process. The fourth stage is known as methanogenesis (methane formation stage) while acetogenesis and methanogenesis are closely connected in the last two stages, involving syntrophic associations between hydrogen-producing acetogenic bacteria and hydrogenotrophic methanogens.

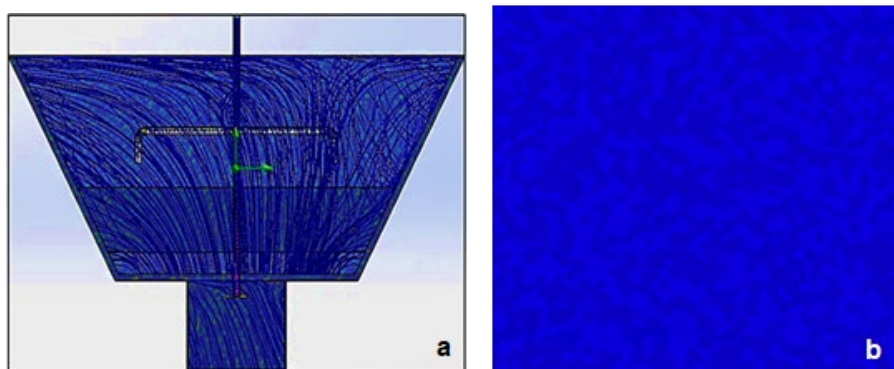


Figure 7. Models of landfill system at inactive state. **a.** Gas pressure, **b.** mass flow rate

The main classification of substrates for methane production includes splitting of acetate, CO_2 reduction with H_2 or formate and rarely ethanol or secondary alcohols as electron donors and reduction in methyl groups of methylated compounds such as methanol, methylated amines or methylated sulphides while methanogenic pathways with respect to each of these classifications include acetoclastic/acetotrophic methanogenesis, hydrogenotrophic methanogenesis as well as hydrogen dependent and hydrogen-independent methylotrophic methanogenesis (Hedderich and Whitman, 2006; Borrel et al., 2013). Acetate is a significant intermediate product in the process of anaerobic digestion of biodegradables to CH_4 and CO_2 , as it can be directly converted to CH_4 and CO_2 via acetoclastic methanogens or syntrophically oxidize to H_2 and CO_2 (Schink & Stamms, 2006).

Landfill gas is the outcome of three processes including the evaporation of volatile organic compounds such as solvents, chemical and biological reaction between waste substrates as well as microbial activities particularly methanogenesis. While the first two processes depend majorly on the waste characteristics, the dominant process in landfill systems is the third process where organic waste is broken down by anaerobic bacteria to produce biogas which comprises CH_4 , CO_2 and traces of other compounds (Ebunilo et al., 2018; Ikpe et al., 2019). Despite the heterogeneity of landfilled waste matrix, the evolution of gas across unsaturated porous media maintains a specific kinematic pattern which involves flow from a region of saturated and semi-saturated porous media to a region of unsaturated porous media. It also involves flow from a region of higher temperature and pressure to a region of lower temperature and pressure. This is because, higher and optimum temperature accelerates organic waste decomposition for rapid production of landfill gas.

Figure 8a represents landfill gas pressure trajectories at anaerobic digestion temperature of 305K. The maximum landfill gas pressure at anaerobic digestion temperature of 305K is observed as 14.40 Kpa. The gas pressure trajectories shows the pressure flowing towards the perforated holes on the gas extraction pipe and the upper section of the landfill which is not porous and not saturated by the upflowing gas. The upper section of the landfill (which can also be considered as a mini gas holder) and the gas extraction channels are completely empty and less saturated. Thus, landfill gas evolving from the anaerobic digestion process flows from high pressure regions to low pressure regions in the porous waste media and when saturated, flows upward to occupy the space at the upper section of the waste layer prior to evacuation. Figure 8b shows the mass flow rate of landfill gas at anaerobic digestion temperature of 305K, implying that with anaerobic digestion temperature of 305K, maximum mass flow rate of $1\text{E-}07$ Kg/s is obtained. landfill gas due to the presence of other gases, the mass flow rate of landfill gas is described as a large number of different microscopic atomic or molecular particles (the mass densities are different because gases have different masses per particle) flowing in constant, rapid random motion within the boundary walls of the landfill system. Hence, the density of landfill gas is

described as the mass of gas occupying the landfill volume at a specified temperature and pressure. Mass flow rate of the gas particles intensify with higher pressures, causing the gas particles to undergo random elastic collisions with one another and with the boundary walls of the system.

Figure 8c shows landfill gas pressure for various flow distances at landfill anaerobic temperature of 305 K. Maximum landfill gas pressure obtained at low, intermediate and high pressure zones within the landfill confinements were 6.81, 11.4 and 14.4 with an average of 10.87 KPa along maximum flow distance of 0.045 m. The plot indicates that the migration of landfill gas within the boundary walls of the system is characterized by brownian motion resulting from random movement of suspended gas particles in the landfill system. The pattern of motion is typically characterized by random fluctuations along a particle's position within sub-domain of the fluid (landfill gas) followed by a variational movement to another sub-domain. Each movement is followed by further fluctuations within the boundary walls of the new enclosed volume. Consequently, direction of the force of atomic bombardment changes constantly, and at different intervals, the particles are hit more on one side than another, resulting in random nature of the motion exhibited by the gas particles. As indicated by the plot in Figure 8c, the gas movement does not have a specific or preferential direction of flow, and the pattern describes the landfill gas under thermal equilibrium, as the temperature within each domain and sub-domain is spatially uniform and temporally constant. In this context, the overall linear and angular momentum of the gas remains null over time. Therefore, the kinetic energies of the molecular brownian motions, alongside those of molecular rotations and vibrations sum up to the calorific component of the gas's internal energy.

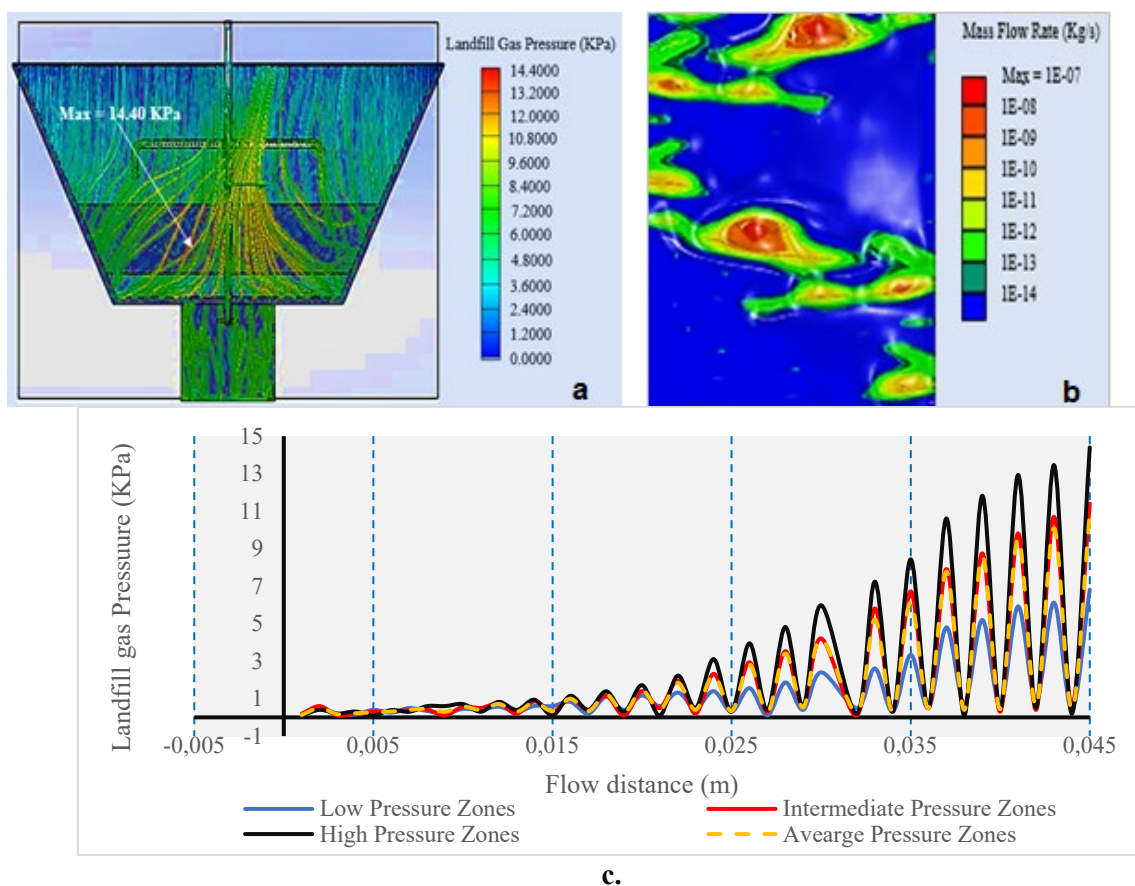


Figure 8. a. Landfill gas pressure at anaerobic digestion temperature of 305K, b. Mass flow rate at anaerobic digestion temperature of 305K, c. Plot of landfill gas pressure against the flow distance

Figure 9a represents landfill gas pressure trajectories at anaerobic digestion temperature of 309K. The maximum landfill gas pressure at anaerobic digestion temperature of 309K is observed as 16.80 Kpa. Figure 9b shows the mass flow rate of landfill gas at anaerobic digestion temperature of 309K, implying that with anaerobic digestion temperature of 309K, maximum mass flow rate of 1E-06 kg/s is obtained. Figure 9c shows landfill gas pressure for various flow distances at the same landfill anaerobic

temperature of 309 K. The maximum landfill gas pressure obtained at low, intermediate and high pressure zones within the landfill confinements were 7.9, 15.24 and 16.8 with an average of 13.31 KPa along maximum flow distance of 0.045 m. The results indicate that the maximum landfill gas pressure and mass flow rate are higher at anaerobic digestion temperature of 309K than anaerobic temperature of 305K reported previously. Similarly, the maximum landfill gas pressure obtained at low, intermediate and high pressure zones within the landfill confinements were also higher than those reported previously for anaerobic temperature of 305K.

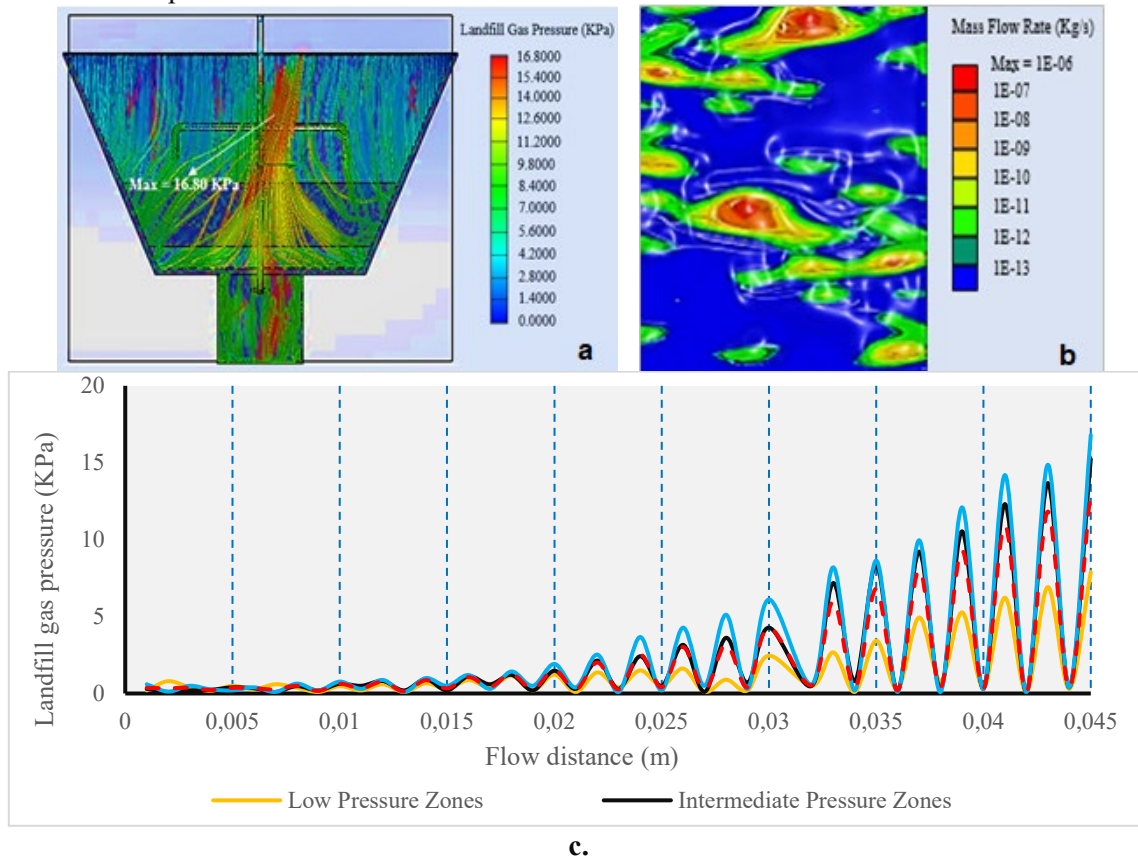


Figure 9. a. Landfill gas pressure at anaerobic digestion temperature of 309K, b. Mass flow rate at anaerobic digestion temperature of 309K, c. Plot of landfill gas pressure against the flow distance

Figure 10a represents landfill gas pressure trajectories at anaerobic digestion temperature of 313K. The maximum landfill gas pressure at anaerobic digestion temperature of 313K is observed as 19.20 Kpa while a maximum mass flow rate of 1E-05 Kg/s was obtained at anaerobic digestion temperature of 313K in Figure 10b. Landfill gas pressure for various flow distances at landfill anaerobic temperature of 313K is shown in Figure 10c, where maximum landfill gas pressure at low, intermediate and high pressure zones within the landfill confinements were recorded as 9.42, 17.4 and 19.18 with an average of 15.3 KPa along maximum flow distance of 0.045 m. The results indicate that the maximum landfill gas pressure and mass flow rate are higher at anaerobic digestion temperature of 313K than anaerobic temperature of 309K reported previously. Similarly, the maximum landfill gas pressure obtained at low, intermediate and high pressure zones within the landfill confinements were also higher than those reported previously for anaerobic temperature of 309K.

Figure 11a represents landfill gas pressure trajectories at anaerobic digestion temperature of 317K. At anaerobic digestion temperature of 317K, the maximum landfill gas pressure was observed as 22.80 Kpa while the maximum mass flow rate of 1E-03 Kg/s was obtained at anaerobic digestion temperature of 309K in Figure 11b. Landfill gas pressure for various flow distances at anaerobic temperature of 317K is shown in Figure 11c, indicating maximum landfill gas pressure at low, intermediate and high pressure zones within the landfill confinements as 11.87, 18.98 and 22.63 with an average of 17.8 KPa across 0.045 m maximum flow distance. From the results aforementioned, maximum landfill gas pressure and mass flow rate are higher at anaerobic digestion temperature of 317K than anaerobic

temperature of 313K reported previously. Similarly, the maximum landfill gas pressure obtained at low, intermediate and high pressure zones within the landfill confinements were also higher than those reported previously for anaerobic temperature of 313K.

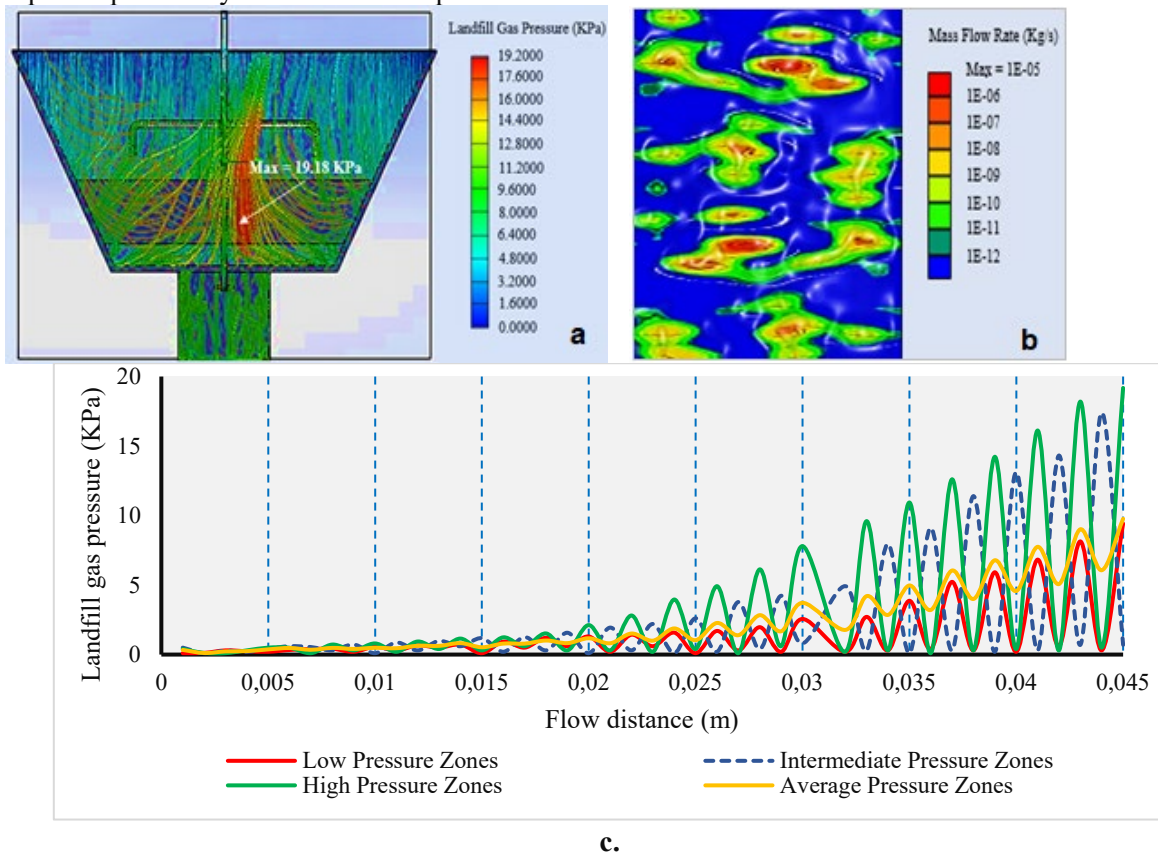


Figure 10. a. Landfill gas pressure at anaerobic digestion temperature of 313K, b. Mass flow rate at anaerobic digestion temperature of 313K, c. Plot of landfill gas pressure against the flow distance

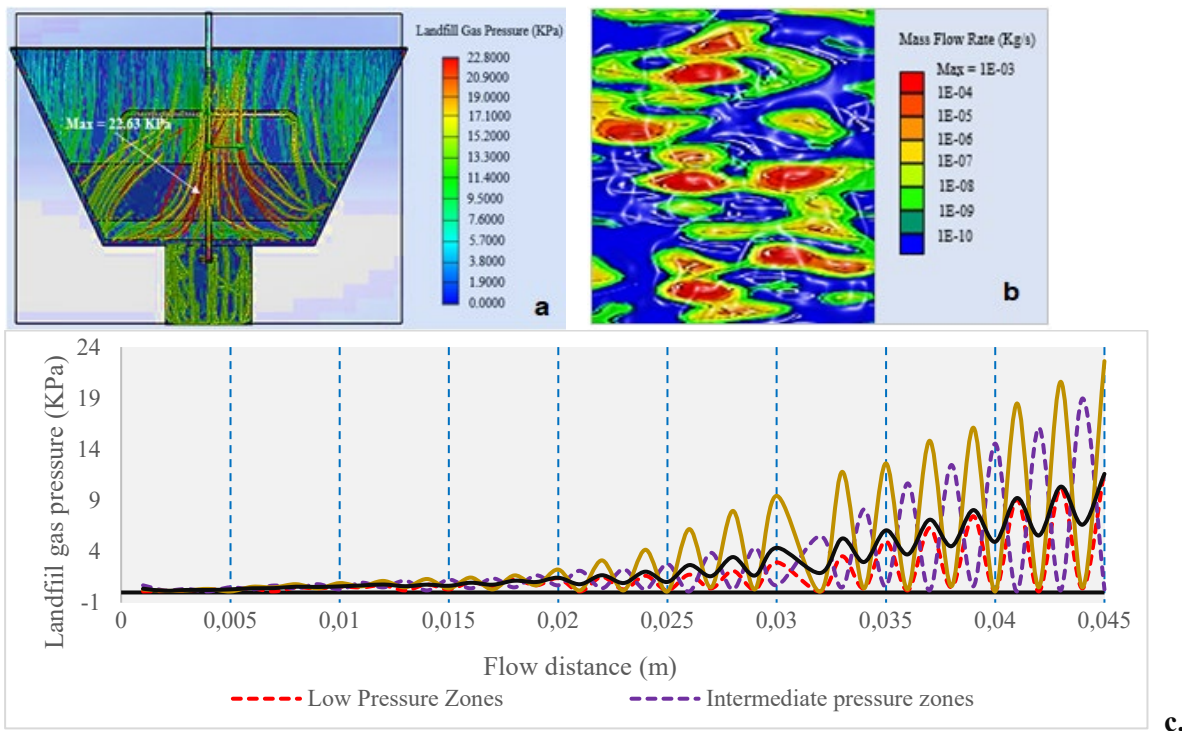


Figure 11. a. Landfill gas pressure at anaerobic digestion temperature of 317K, b. Mass flow rate at anaerobic digestion temperature of 317K, c. Plot of landfill gas pressure against the flow distance

Figure 12a represents landfill gas pressure trajectories at anaerobic digestion temperature of 321K. At anaerobic digestion temperature of 321K, the maximum landfill gas pressure was observed as 25.20 Kpa while the maximum mass flow rate of 1E-01 Kg/s was obtained at anaerobic digestion temperature of 309K in Figure 12b. Landfill gas pressure for various flow distances at anaerobic temperature of 321K is shown in Figure 12c, indicating maximum landfill gas pressure at low, intermediate and high pressure zones within the landfill confinments as 14.71, 21.63 and 24.86 with an average of 20.4 KPa along 0.045 m maximum flow distance. From the results aforementioned, maximum landfill gas pressure and mass flow rate are higher at anaerobic digestion temperature of 321K than anarobic temperature of 317K reported previously. Similarly, the maximum landfill gas pressure obtained at low, intermediate and high pressure zones within the landfill confinments were also higher than those previously mentioned for anarobic temperature of 317K.

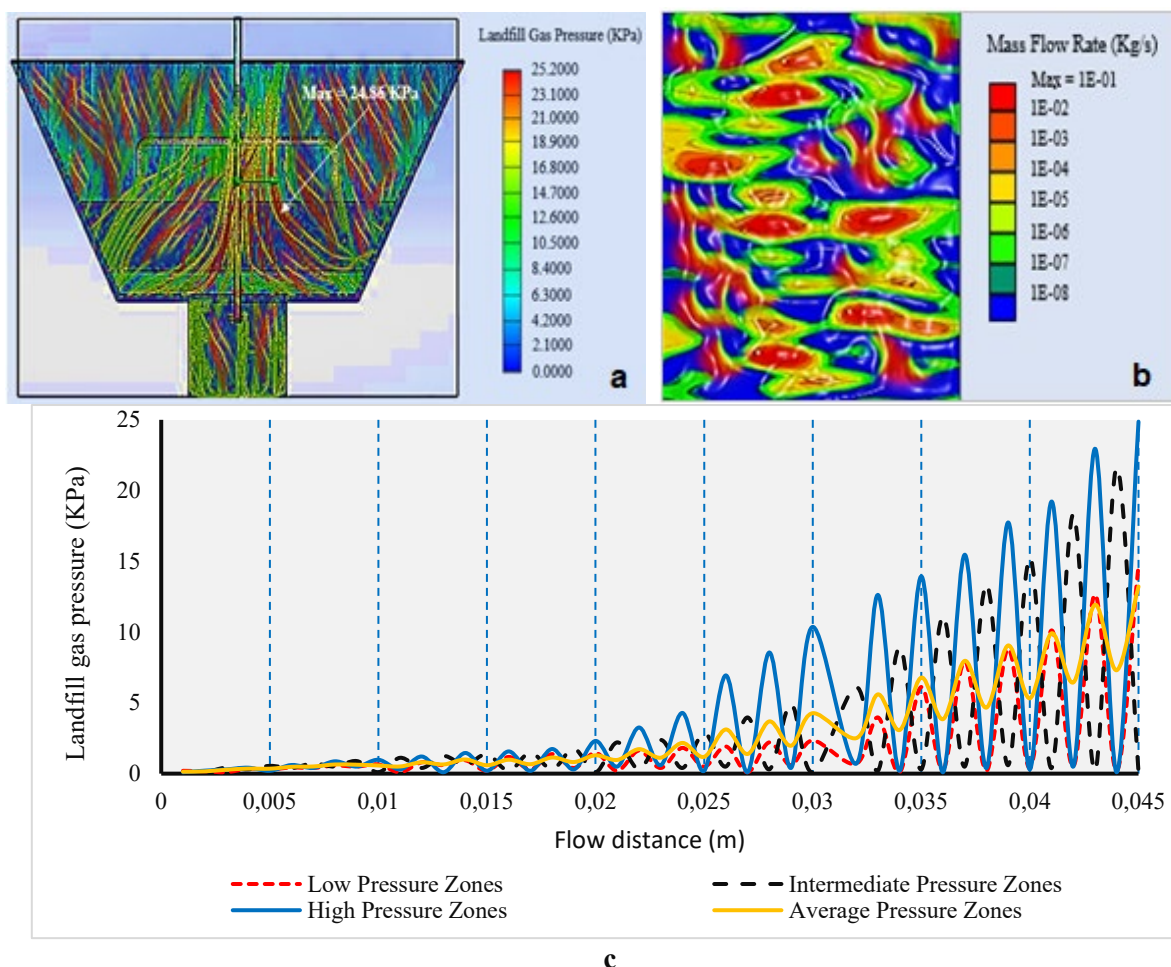


Figure 12. a. Landfill gas pressure at anaerobic digestion temperature of 321K, b. Mass flow rate at anaerobic digestion temperature of 321K, c. Plot of landfill gas pressure against the flow distance

Conclusion

In this study, the kinetics of anaerobic digestion temperature regime in relation to multiphase flow across unsaturated porous organic waste media in a prototype landfill design framework was successfully modelled. It was observed that moles of the landfill gas per unit flow rate were much with higher pressures compared to lower pressures which only had few moles of gas per unit flow rate. This is because at higher pressure, mass flow rate of the landfill gas increases significantly, and in the process carries a large number of gas particles which represents mole density of the landfill gas flowing per unit area across the unsaturated porous waste media. Findings from this study also reveal that multiphase flow of landfill gas is a function of the temperature and heat distribution rate across the unsaturated porous waste media. Therefore, optimum temperature within the landfill system accelerates the rate of heat distribution and microbial activities (breaking down of organic substrate) for proper decomposition

of organic fraction of waste within each layer in the landfill system. Although semi-saturated and saturated porous waste media was not fully analysed in this study, it is deduced from the models developed that landfill gas pressure and mass flow rate in the unsaturated media is higher than both parameters in semi-saturated and saturated porous waste media. However, landfill gas pressure and mass flow rate in the semi-saturated media is higher than both parameters in the saturated porous waste media which appears to be almost impervious. Hence, engineered landfill system designed for gas production should be managed as unsaturated porous media for effective gas recovery.

References

- Kjeldsen P, Fischer EV, (1995) Landfill gas migration-field investigations at Skellingsted landfill, Denmark. *Waste Management and Resource*, **13**(5), 467-484 (1995). <https://doi.org/10.1177/0734242X9501300>
- Spokas KA, Bogner JE, (1996) Field system for continuous measurement of landfill gas pressures and temperatures. *Waste Management and Resource*, **14**(3), 233-242. https://www.ars.usda.gov/ARSUserFiles/41695/Updates/1996_SpokasFieldSystemsFor.pdf
- Bentley HW, Smith SJ, Tang J, Walter GR, (2003) A method for estimating the rate of landfill gas generation by measurement and analysis of barometric pressure waves. In: Proceedings of the 18th International Conference on Solid Waste Technology and Management, Philadelphia, USA. <http://hgcinc.com/a%20method%20measure%20rate%20LFG%201-14-03%20HB.pdf>
- Orhorhoro EK, Ikpe AE, Ukwaba SI, (2018) Effects of Landfill Gas Flow Trajectories at Three Distinct Temperature Phases on the Stress-Strain-Displacement Properties of a Gas Extraction Pipe. *Journal of Applied Science and Environmental Management*, **22**(11), 1737-1743. DOI:[10.4314/jasem.v22i11.5](https://doi.org/10.4314/jasem.v22i11.5)
- Gebert J, Groengroeft A, (2006) Passive landfill gas emission-influence of atmospheric pressure and implications for the operation of methane-oxidising biofilters. *Waste Management*, **26**(3), 245-251. <https://doi.org/10.1016/j.wasman.2005.01.022>
- Chen ZK, Coo JL, Ng CW, (2016) Experimental study of gas breakthrough and emission in an unsaturated clay landfill cover. E3S Web of Conferences, 9, 13005. DOI:[10.1051/e3sconf/20160913005](https://doi.org/10.1051/e3sconf/20160913005)
- Nec Y, Huculak G, (2010) Landfill gas flow: collection by horizontal wells. Thompson Rivers University, Kamloops, British Columbia, Canada. <https://doi.org/10.1007/s11242-019-01338-3>
- Zhang T, Shi JY, Qian XD, Ai YB, (2019) Temperature and gas pressure monitoring and leachate pumping tests in a newly filled MSW layer of a landfill. *International Journal of Environmental Resources*, **13**(1), 1-19. <https://doi.org/10.1007/s41742-018-0157-0>
- Ikpe, A.E, Ndon AE, Etim PJ, (2020a) A Conceptual Framework for Bio-thermal variations in Municipal Solid Waste Landfill under Mesophilic Temperature Regime. *International Journal of Computational and Experimental Science and Engineering*, **6**(3), 152-164. DOI:[10.22399/ijcesen.737662](https://doi.org/10.22399/ijcesen.737662)
- Ikpe AE., Ndon AE, Etim PJ, (2020b) Fuzzy Modelling and Optimization of Anaerobic Co-Digestion Process Parameters for Effective Biogas Yield from Bio-Wastes. *The International Journal of Energy & Engineering Sciences*, **5**(2), 43-61. <https://dergipark.org.tr/en/download/article-file/1161518>
- Feng Q, Liu L, Xue Q, Zhao Y, (2009) Landfill Gas Generation and Transport in Bioreactor Landfill. Proceedings of International Symposium on Geoenvironmental Engineering, 633-636, September 8-10, Hangzhou, China. https://doi.org/10.1007/978-3-642-04460-1_68
- Ikpe AE, Ndon AE, Etuk EM, (2020c) Parametric Study of Polypropylene Based Geotextile Mat for Optimum Performance in Engineered Landfill Systems. *Applications of Modelling and Simulation*, **4**, 149-158. https://arqiipubl.com/ojs/index.php/AMS_Journal/article/view/131/90.
- Ikpe AE, Ndon AE, Adoh AU. (2019) Modelling and Simulation of High Density Polyethylene Liner Installation in Engineered Landfill for Optimum Performance. *Journal of Applied Science and Environmental Management*, **23**(3), 449-456. DOI: [10.4314/jasem.v23i3.13](https://doi.org/10.4314/jasem.v23i3.13).
- Ebunilo PO, Okovido J, Ikpe AE, (2018) Investigation of the energy (biogas) production from co-digestion of organic waste materials. *International Journal of Energy Applications and Technologies*, **5**(2), 68-75. DOI:[10.31593/ijeat.417498](https://doi.org/10.31593/ijeat.417498).

- Lefebvre X, Lanini S, Houi D, (2000) The role of aerobic activity on refuse temperature rise, I. Landfill experimental study. *Waste Management and Resources*, **18**(5), 444-452. <https://doi.org/10.1177/0734242X0001800505>.
- Jang YS, Kim YI, (2003) Behaviour of a municipal landfill from field measurement data during a waste-disposal period. *Environmental Earth Sciences*, **44**(5), 592–598. <https://doi.org/10.1007/s00254-003-0796-z>
- Hedderich R, Whitman WB, (2006) Physiology and Biochemistry of Methane-Producing Archaea. In Dworking, M. editor. *The Prokaryotes*, 3rd Edition, Springer, Berlin, Heidelberg. https://doi.org/10.1007/978-3-642-30141-4_81
- Ikpe AE, Imonitie DI, Ndon, AE, (2019) Investigation of Biogas Energy Derivation from Anaerobic Digestion of Different Local Food Wastes in Nigeria. *Academic Platform Journal of Engineering and Science*, **7**(2), 332-340. [Doi: 10.21541/apjes.441166](https://doi.org/10.21541/apjes.441166)
- Borrel G, Toole PW, Harris H, Peyeret P, Brugere JF, Gribaldo S, (2013) Phylogenomic Data Support a Seventh Order of Methylophilic Methanogens and Provide Insights into the Evolution of Methanogenesis. *Genome Biology and Evolution*, **5**(10), 1769-1780. [DOI: 10.1093/gbe/evt128](https://doi.org/10.1093/gbe/evt128)
- Buivid MG, Wise DL, Blanchet MJ, Remedios EC, Jenkins BN, Boyd WF, Pacey JG, (1981) Fuel gas enhancement by controlled landfilling municipal solid waste. *Resource and Conservation*, **6**(1), 3-20. [https://doi.org/10.1016/0166-3097\(81\)90003-1](https://doi.org/10.1016/0166-3097(81)90003-1).
- Li YC, Cleall PJ, Ma XF, Zhan TL, Chen YM, (2012) Gas pressure model for layered municipal solid waste landfills. *Journal of Environmental Engineering*, **138**(7), 752-760. [DOI:10.1061/\(ASCE\)EE.1943-7870.0000533](https://doi.org/10.1061/(ASCE)EE.1943-7870.0000533).
- Li YC, Zheng J, Chen YM, Guo RY, (2013) One-dimensional transient analytical solution for gas pressure in municipal solid waste landfills. *Journal of Environmental Engineering*, **139**(12), 1441-1445. [DOI:10.1061/\(ASCE\)EE.1943-7870.0000759](https://doi.org/10.1061/(ASCE)EE.1943-7870.0000759)
- Khalil MJ, Gupta R, Sharma K, (2014) Microbiological Degradation of Municipal Solid Waste in Landfills for LFG Generation. *International Journal of Engineering and Technical Research*, **2321**, 10-14. https://www.erpublishing.org/published_paper/IJETR-APRIL-2014-STET-03.pdf
- Lu S, Xiong J, Feng S, Chen H, Bai Z, Fu W, Lu F, (2019) A finite-volume numerical model for bio-hydro-mechanical behaviours of municipal solid waste in landfills. *Computers and Geotechnics*, **109**, 204-219. <https://doi.org/10.1016/j.compgeo.2019.01.012>.
- Nastev M, Therrien R, Lefebvre R, Gélinas P, (2001) Gas production and migration in landfills and geological materials. *Journal of Contaminant Hydrology*, **52**(1-4), 187–211. [DOI: 10.1016/S0169-7722\(01\)00158-9](https://doi.org/10.1016/S0169-7722(01)00158-9).
- Liu H, Luo X, Jiang X, Cui C, Huyan Z, (2021) The Evaluation System of the Sustainable Development of Municipal Solid Waste Landfills and Its Application. *Sustainability*, **13**(1150), 1-17. [DOI:10.3390/su13031150](https://doi.org/10.3390/su13031150).
- Haug RT, (1993) *The Practical Handbook of Compost Engineering*. 1st Edition, Lewis Publishers, New York, USA. <https://doi.org/10.1201/9780203736234>
- Poling, B. E., Prausnitz, J. M., O'Connell, J. P. (2001) *The Properties of Gases And Liquids*. 5th Edition, McGraw-Hill, New York. [DOI: 10.1036/0070116822](https://doi.org/10.1036/0070116822)
- Durmusoglu E, (2002) Landfill settlement with refuse decomposition and gas generation. PhD dissertation, Texas A&M University, College Station. [DOI: 10.1061/\(ASCE\)0733-9372](https://doi.org/10.1061/(ASCE)0733-9372)
- Zhang T, Shi J, Wu X, Lin H, Li X, (2021) Simulation of Gas Transport in A Landfill with Layered New and Old Municipal Solid Waste. *Scientific Report*, **11**, 9436-9449. <https://doi.org/10.1038/s41598-021-88858-5>.
- Baptista M, Antunes F, Souteiro GM, Morvan B, Silveira A, (2010) Composting kinetics in full-scale mechanical-biological treatment plants. *Waste Management*, **30**(10), 1908-1921. <https://doi.org/10.1016/j.wasman.2010.04.027>.
- Zeng HY, Diao NR, Fang ZH, (2002) A finite line-source model for boreholes in geothermal heat exchangers. *Heat Transfer-Asian Research*, **31**(7), 558-567. [DOI:10.1002/htj.10057](https://doi.org/10.1002/htj.10057).
- Yang Y, (2016) Analyses of Heat Transfer and Temperature-induced Behaviour in Geotechnics. Ruhr-University, Bochum, Germany. https://www.bgu.ruhr-uni-bochum.de/bgu/mam/dissertation_yang2016.pdf
- Nield D, Bejan A, (2006) *Convection in porous media*, 3rd Edition. Berlin, Springer, 2006. [DOI:10.1007/0-387-33431-9](https://doi.org/10.1007/0-387-33431-9).

- Sole-Mauri F, Illa J, Magrí A, Prenafeta-Boldú FX, Flotats X, (2007) An integrated biochemical and physical model for the composting process. *Bioresource Technology*, **98**(17), 3278-3293. <https://doi.org/10.1016/j.biortech.2006.07.012>
- Schink B, Stamms AJ, (2006) Syntrophism among Prokaryotes. In: Dworkin M., Editor. *The Prokaryotes*, 3rd Edition, p. 309-335, Springer-Verlag, New York. DOI: [10.1007/0-387-30742-7_11](https://doi.org/10.1007/0-387-30742-7_11).
- Mason IG, (2009) Predicting biodegradable volatile solids degradation profiles in the composting process. *Waste Management*, **29**(2), 559-569. DOI: [10.1016/j.wasman.2008.05.001](https://doi.org/10.1016/j.wasman.2008.05.001)
- Lin YP, Huang GH, Lu HW, He L, (2008) Modelling of substrate degradation and oxygen consumption in waste composting processes. *Waste Management*, **28**(8), 1375-1385. <https://doi.org/10.1016/j.wasman.2007.09.016>.
- Qin X, Huang G, Zeng G, Chakma A, Xi B, (2007) A fuzzy composting process model. *Journal of Air and Waste Management Association*, **57**(5), 535-550. <https://doi.org/10.3155/1047-3289.57.5.535>.
- Bear J, (1972) *Dynamics of Fluids in Porous Media*. Dover Publications Inc, New York, ISBN: 0-486-65675-6. <https://lib.ugent.be/en/catalog/rug01:000487153>.
- Staub M, Galiotti B, Oxarango L, Khire MV, Gourc JP, (2009) Porosity and hydraulic conductivity of MSW using laboratory-scale tests. In: Third International Conference of Hydro-Physico-Mechanics of Landfills, Braunschweig, Germany, 10-13 March. <http://ce561.ce.metu.edu.tr/files/2013/11/hydraulic-conductivity-waste-2.pdf>.
- Beaven RP, Powrie W, (1995) Determination of the hydrogeological and geotechnical properties of refuse using a large-scale compression cell. In: Sardinia 1995, Fifth International Landfill Symposium, S. Margherita di Pula, Cagliari, Italy, 2-6 October. file:///C:/Users/Victor%20Etok%20Udo/Downloads/docksci.com_sardinia-95-fifth-international-landfill-symposium.pdf.
- Higgins CW, Walker LP, (2001) Validation of a new model for aerobic organic solids decomposition: simulations with substrate specific kinetics. *Process Biochemistry*, **36**, 875-884. [https://doi.org/10.1016/S0032-9592\(00\)00285-5](https://doi.org/10.1016/S0032-9592(00)00285-5).
- Nayagum D, White J, Rees-White T, Holmes D, Zardava K, (2009) Modelling study of field-scale aerobic treatment of waste using forced-air injection. In: Sardinia 2009, Twelfth International Waste Management and Landfill Symposium, S. Margherita di Pula, Cagliari, Italy, 5-9 October. https://www.tib.eu/en/search/id/TIBKAT:624628027/SARDINIA-2009-Twelfth-International-WasteManagement?tx_tibsearch_search%5Bsearchspace%5D=tibub&cHash=1586f2b8aa9051e74d21e124bebf415a.
- Stegenta-Dabrowska S, Randerson PF, Białowiec A, (2022) Aerobic Biostabilization of the Organic Fraction of Municipal Solid Waste-Monitoring Hot and Cold Spots in the Reactor as a Novel Tool for Process Optimization. *Materials*, **15**(9), 1-18. <https://doi.org/10.3390/ma15093300>
- Iannelli R, Giraldi D, Pollini M, Russomanno F, (2005) Effect of pure oxygen injection as an alternative to air and oxygen-enriched air in the composting processes. In: Sardinia 2005, Tenth International Waste Management and Landfill Symposium, S. Margherita di Pula, Cagliari, Italy, 3-7 October. <https://docplayer.net/31326623-Sardinia-tenth-international-waste-management-and-landfill-symposium-3-7-october-s-margherita-di-pula-cagliari-sardinia-italy.html>.
- Komilis D, Evangelou A, Giannakis G, Lymperis C, (2012) Revisiting the elemental composition and the calorific value of the organic fraction of municipal solid wastes. *Waste Management*, **32**(3), 372–381. <https://doi.org/10.1016/j.wasman.2011.10.034>.
- Rosso L, Lobry JR, Flandrois JP, (1993) An unexpected correlation between cardinal temperatures of microbial growth highlighted by a new model. *Journal of Theoretical Biology*, **162**, 447-463. [doi:10.1006/jtbi.1993.1099](https://doi.org/10.1006/jtbi.1993.1099)
- Mavridis S, Voudrias EA, (2021) Using biogas from municipal solid waste for energy production: Comparison between anaerobic digestion and sanitary landfilling. *Energy Conversion and Management*, **247**(9), 114613. <https://doi.org/10.1016/j.enconman.2021.114613>
- Fytanidis DK, Voudrias AE, (2014) Numerical simulation of landfill aeration using computational fluid dynamics. *Waste Management*, **34**(4), 804-816. <https://doi.org/10.1016/j.wasman.2014.01.008>
- Mualem Y, (1976) A new model for predicting the hydraulic conductivity of unsaturated porous media. *Water Resources Research*, **12**(3), 513-522. <https://doi.org/10.1029/WR012i003p00513>

- Ranz WE, Marshall WR, (1952) Evaporation from drops, Part I: *Chemical Engineering Progress*, **48** (3), 141-146. <http://dns2.asia.edu.tw/~ysho/YSHOEnglish/2000%20CE/PDF/Che%20Eng%20Pro48,%20141.pdf>
- van Genuchten MT, (1980) A closed form equation for predicting the hydraulic conductivity of unsaturated soils. *Soil Science Society of America Journal*, **44**(5), 892-898. [DOI:10.2136/sssaj1980.03615995004400050002x](https://doi.org/10.2136/sssaj1980.03615995004400050002x).
- Sikora A, Detman A, Chojnacka A, Blaszczyk MK, (2017) *Fermentation Processes*. IntechOpen Limited, UK. [DOI:10.5772/61924](https://doi.org/10.5772/61924).